



COLLÈGE  
DE FRANCE  
—1530—

Chaire de Physique  
de la Matière Condensée  
Antoine Georges

# Réseaux de Neurones, Apprentissage et Physique Quantique

Cours 4:

Représentations d'états quantiques fermioniques  
utilisant les réseaux de neurones

I – Introduction aux fonctions d'ondes variationnelles

Cycle 2022-2023  
23 mai 2023



COLLÈGE  
DE FRANCE  
— 1530 —

Chaire de Physique  
de la Matière Condensée  
Antoine Georges

# Machine Learning and Neural Networks for Quantum Physics

Lecture 4

Fermionic Quantum States with Neural Networks  
I – An Introduction to Variational Wave Functions

Cycle 2022-2023  
May 23, 2023

# Seminar (11h30): Juan Carrasquilla *Quantum States with Neural Networks: Representations and Tomography*



## ***Quantum States with Neural Networks: Representations and Tomography***

Juan Felipe Carrasquilla Álvarez  
*Vector Institute, Toronto*

In this presentation I will discuss representations of quantum states which take inspiration from architectures developed by computer vision and natural language processing communities. I will discuss in particular convolutional neural networks and recurrent neural networks and show applications of these architectures in the context of ground state estimation and quantum state tomography.

# Mailing List

(Weekly announcement of lecture and seminar, etc.)

Send email to: [listes-diffusion.cdf@college-de-france.fr](mailto:listes-diffusion.cdf@college-de-france.fr)

Subject line: subscribe chaire-pmc.ipcdf

...or: unsubscribe chaire-pmc.ipcdf

You can also just send me an email to be placed on the list

## Website:

<https://www.college-de-france.fr/site/antoine-georges/index.htm>

Lectures are video recorded  
and available on the website

Part of today's lecture will be done on the board.

Slides will be used occasionally to show data, references, etc.

For full lecture, see video.

# Menu of the day:

- The many fermion problem: introduction, notations
- Some classic variational wave functions: Slater determinant, BCS/pairs, Gutzwiller, Jastrow-Slater, Backflow, ...
- Optimizing wave functions with Monte Carlo
- How ML/neural networks are transforming the field: overview
- Hidden Fermion Determinantal States and some other NQS for fermions → Lecture 5

# Some useful general references on variational wave-functions:

- Federico Becca *'Variational wavefunction for strongly correlated fermionic systems'* in Jülich lectures Vol 9 (2019) <http://www.cond-mat.de/events/correl19>
- Federico Becca and Sandro Sorella *'Quantum Monte Carlo Approaches for Correlated Systems'* Cambridge University Press, 2017
- Also some older refs:
- Dieter Vollhardt *Variational wavefunctions for correlated lattice fermions* (Bookchapter, NATO series, 1988)
- Claudius Gros *'Physics of projected wavefunctions'* Annals of Physics 189, 53 (1989)

# Interacting Fermions: Models and Materials

- Lattice Models:
  - Spinless fermions with n.n interactions
  - Hubbard model
- Continuum space:
  - Helium 3
  - Electron Gas
- Molecules and Materials can be described either directly in the continuum or using a basis set

# The 2-site Hubbard Model

cf. 2021 Lectures

$$\hat{H} = -t \sum_{\sigma} \left[ c_{1\sigma}^{\dagger} c_{2\sigma} + \text{h.c.} \right] + U \left[ \hat{n}_{1\uparrow} \hat{n}_{1\downarrow} + \hat{n}_{2\uparrow} \hat{n}_{2\downarrow} \right]$$

Symmetries: Separate conservation of number of up- and down-spin particles, spin conservation and parity (exchange of *lattice sites* 1 and 2) - note that  $S^z = (N_{\uparrow} - N_{\downarrow})/2$  so we can just consider  $N$  and  $S^z$  equivalently to  $N_{\uparrow}, N_{\downarrow}$ .

$$[H, N_{\uparrow}] = [H, N_{\downarrow}] = [H, \mathbf{S}^2] = [H, S^z] = [H, P_{12}] = 0 \quad (\text{B2})$$

Hence, we can use quantum numbers  $(N, S, S^z, P)$ .

The total Hilbert space has dimension  $2^4 = 16$ . We discuss the sectors  $N = 0, 1, 2$  (the sector with  $N = 3$  and  $N = 4$  are related by symmetry to that with  $N = 1$  and  $N = 0$ , respectively).

- $N = 0$  (1 state):  $|0\rangle$ ,  $E = 0$
- $N = 1$  (4 states):  $\frac{1}{\sqrt{2}} [|0, \sigma\rangle \pm |\sigma, 0\rangle]$  have  $S^z = \sigma$ ,  $P = \pm$  and hence are eigenstates with  $E = -t, +t$  respectively. A comment is in order here: since these are one-particle states with momenta  $k = 0$  and  $k = \pi$  (bonding and antibonding combinations), one would think of obtaining their energies from  $\varepsilon_k = -2t \cos k$ , leading to  $\pm 2t$ . However, this is valid with periodic boundary conditions. In order to retrieve the open boundary condition result, one has to take half of the hopping in the periodic system, hence  $\pm t$ .

# The N=2 sector (6 states)

S	$S^z$	$P_{12}$	1 <sup>st</sup> quantized	2 <sup>nd</sup> quantized	$P_{ab}$
1	-1	-1	$\frac{1}{\sqrt{2}} [\chi_1(a)\chi_2(b) - \chi_1(b)\chi_2(a)] \otimes  \uparrow\uparrow\rangle$	$c_{1\uparrow}^\dagger c_{2\uparrow}^\dagger  0\rangle$	-1
1	0	-1	$\frac{1}{\sqrt{2}} [\chi_1(a)\chi_2(b) - \chi_1(b)\chi_2(a)] \otimes \frac{1}{\sqrt{2}} [ \uparrow\downarrow\rangle +  \downarrow\uparrow\rangle]$	$\frac{1}{\sqrt{2}} [c_{1\uparrow}^\dagger c_{2\downarrow}^\dagger + c_{1\downarrow}^\dagger c_{2\uparrow}^\dagger]  0\rangle$	-1
1	-1	-1	$\frac{1}{\sqrt{2}} [\chi_1(a)\chi_2(b) - \chi_1(b)\chi_2(a)] \otimes  \downarrow\downarrow\rangle$	$c_{1\downarrow}^\dagger c_{2\downarrow}^\dagger  0\rangle$	-1
0	0	-1	$\frac{1}{\sqrt{2}} [\chi_1(a)\chi_1(b) - \chi_2(a)\chi_2(b)] \otimes \frac{1}{\sqrt{2}} [ \uparrow\downarrow\rangle -  \downarrow\uparrow\rangle]$	$\frac{1}{\sqrt{2}} [c_{1\uparrow}^\dagger c_{1\downarrow}^\dagger - c_{2\uparrow}^\dagger c_{2\downarrow}^\dagger]  0\rangle$	-1
0	0	+1	$\frac{1}{\sqrt{2}} [\chi_1(a)\chi_1(b) + \chi_2(a)\chi_2(b)] \otimes \frac{1}{\sqrt{2}} [ \uparrow\downarrow\rangle -  \downarrow\uparrow\rangle]$	$\frac{1}{\sqrt{2}} [c_{1\uparrow}^\dagger c_{1\downarrow}^\dagger + c_{2\uparrow}^\dagger c_{2\downarrow}^\dagger]  0\rangle$	-1
0	0	+1	$\frac{1}{\sqrt{2}} [\chi_1(a)\chi_2(b) + \chi_1(b)\chi_2(a)] \otimes \frac{1}{\sqrt{2}} [ \uparrow\downarrow\rangle -  \downarrow\uparrow\rangle]$	$\frac{1}{\sqrt{2}} [c_{1\uparrow}^\dagger c_{2\downarrow}^\dagger - c_{1\downarrow}^\dagger c_{2\uparrow}^\dagger]  0\rangle$	-1

The 6 basis states of the N=2 sector organized according to symmetries: S,  $S^z$ ,  $P_{12}$

Note:

- '1st quantized' vs '2<sup>nd</sup> quantized' notations
- Canonical ordering chosen here to be: 1,up; 1,down;2,up;2,down

- $N = 2$  (6 states): This subspace splits into an  $S = 1$  (3 states forming a spin triplet) , and an  $S = 0$  sector (3 states). It is useful to organize the basis states according to spin and parity symmetries, as in Table I. It is also instructive to compare the first- and second-quantized notations for these basis states.

The hamiltonian is diagonal in the triplet sector with eigenvalue  $E = 0$ . Physically, this reflects the fact that the Pauli principle prevents electrons with parallel spin to hop. It is a useful exercise to check that indeed the kinetic energy (hopping) operator acts as  $\hat{T}|\psi_t\rangle = 0$  on all triplet states, which is also guaranteed by the fact that these states have odd parity.

The singlet sector has only one state with odd parity, which is therefore an eigenstate, with energy  $E = U$  (doubly occupied state). Hence, we only have to diagonalize the  $2 \times 2$  block corresponding to the even-parity singlet sector. We have:

$$\hat{T} \frac{1}{\sqrt{2}} [c_{1\uparrow}^\dagger c_{2\downarrow}^\dagger - c_{1\downarrow}^\dagger c_{2\uparrow}^\dagger] |0\rangle = -2t \frac{1}{\sqrt{2}} [c_{1\uparrow}^\dagger c_{1\downarrow}^\dagger + c_{2\uparrow}^\dagger c_{2\downarrow}^\dagger] |0\rangle \quad (\text{B3})$$

Hence the matrix reads, in the basis of the 2 last states in Table I:

$$\begin{pmatrix} U & -2t \\ -2t & 0 \end{pmatrix} \quad (\text{B4})$$

with eigenvalues:

$$E_{\pm} = \frac{1}{2} [U \pm \sqrt{U^2 + 16t^2}] = \frac{U}{2} \left[ 1 \pm \sqrt{1 + \frac{16t^2}{U^2}} \right]$$

and corresponding eigenvectors:

$$|\Psi_{\pm}\rangle = \cos \theta_{\pm} \frac{1}{\sqrt{2}} [c_{1\uparrow}^\dagger c_{1\downarrow}^\dagger + c_{2\uparrow}^\dagger c_{2\downarrow}^\dagger] |0\rangle + \sin \theta_{\pm} \frac{1}{\sqrt{2}} [c_{1\uparrow}^\dagger c_{2\downarrow}^\dagger - c_{1\downarrow}^\dagger c_{2\uparrow}^\dagger] |0\rangle$$

with:

$$\frac{1}{\tan \theta_{\pm}} = -u \left[ 1 \pm \sqrt{1 + \frac{1}{u^2}} \right], \quad u \equiv \frac{U}{4t}$$

In the limit  $U/t \rightarrow 0$ ,  $|\Psi_{-}\rangle$  corresponds to the state in which two electrons occupy the bonding ( $k = 0$ ) state, corresponding to  $\theta_{-} \rightarrow \pi/4$  and  $E_{-} = -2t$  (see comment above about periodic b.c.). Correspondingly,  $|\Psi_{+}\rangle$  corresponds to the state in which two electrons occupy the antibonding ( $k = \pi$ ) state, hence  $E_{+} = +2t$  and  $\theta_{+} \rightarrow -\pi/4$ .

In the opposite limit  $U/t \rightarrow +\infty$ , we have  $E_{+} \sim U$  and  $E_{-} \sim -4t^2/U$  and  $\theta_{+} \rightarrow 0$ ,  $\theta_{-} \rightarrow \pi/2$ . The ground-state is thus  $|\Psi_{-}\rangle$ , which in the large  $U/t$  limit is given by, to order  $1/u^3$ :

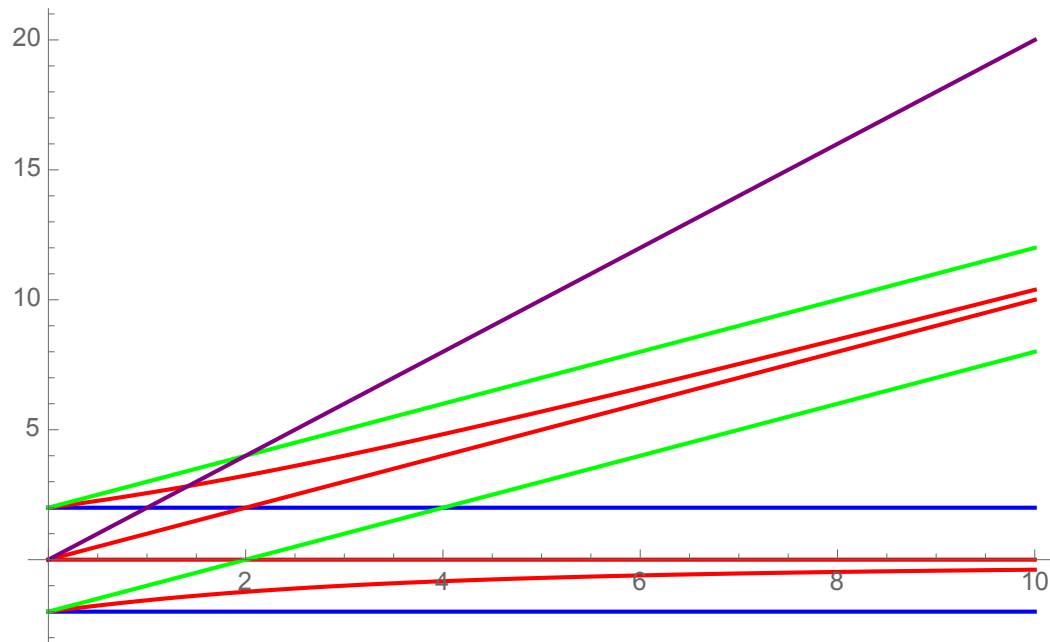
$$|\Psi_{\pm}\rangle = \left(1 - \frac{1}{8u^2}\right) \frac{1}{\sqrt{2}} \left[ c_{1\uparrow}^{\dagger} c_{2\downarrow}^{\dagger} - c_{1\downarrow}^{\dagger} c_{2\uparrow}^{\dagger} \right] |0\rangle + \frac{1}{2u} \frac{1}{\sqrt{2}} \left[ c_{1\uparrow}^{\dagger} c_{1\downarrow}^{\dagger} + c_{2\uparrow}^{\dagger} c_{2\downarrow}^{\dagger} \right] |0\rangle \quad (\text{B8})$$

The ground-state is dominantly the singlet configuration of two electrons on distinct sites, with a small  $\sim 1/u$  admixture of the doubly occupied state on either site. As compared to the triplet state with  $E = 0$ , the ground-state is lower in energy by the antiferromagnetic superexchange:

$$\Delta E = \frac{4t^2}{U} \equiv J \quad (\text{B9})$$

The low-energy sector for  $U \gg t$  comprises four states: this singlet state and the triplet. Hence, it can be described as a spin-only effective hamiltonian:

$$\hat{H}_{\text{eff}} = J \left( \mathbf{S}_1 \cdot \mathbf{S}_2 - \frac{1}{4} \right) \quad (\text{B10})$$



2-sites:  
 ← All energy levels  
 vs.  $U/t$

Note: continuity between the  $U=0$  and the large- $U$  ground-state

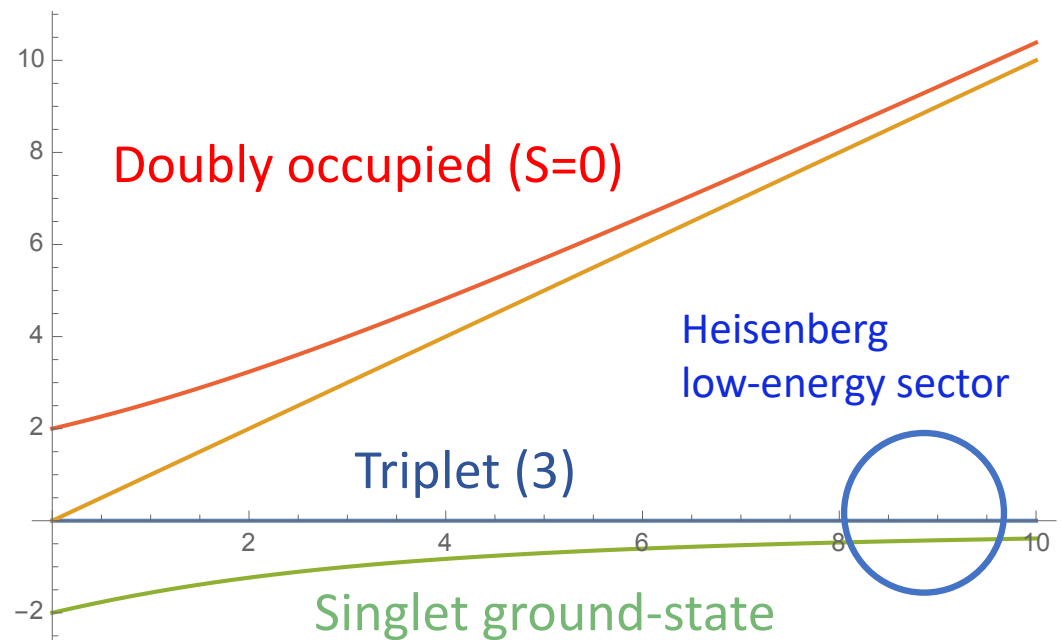
cf.  $H_2$  molecule

From 2 electrons in bonding state

(Hartree-Fock-Slater)

to Heitler-London

(= chemical bond!)



# Slater Determinants and the Hartree-Fock Approximation

$$\begin{aligned}\Psi_{\text{SD}}(1, \dots, N) &= \det [\phi_{\alpha_i}(j)] \\ &= \sum_{\sigma} \varepsilon_{\sigma} \phi_{\alpha_{\sigma(1)}}(1) \cdots \phi_{\alpha_{\sigma(N)}}(N)\end{aligned}$$

$$|x\rangle \equiv |p_1, \dots, p_N\rangle = \varepsilon_{\sigma(x)} |n(x)\rangle$$

$$|\Psi_{\text{SD}}\rangle = \sum_n \psi_{\text{SD}}(n) |n\rangle = \frac{1}{N!} \sum_x \psi_{\text{SD}}(x) |x\rangle$$

$$\psi_{\text{SD}}(x) = \varepsilon_{\sigma(x)} \psi[n(x)] = \det \begin{pmatrix} \Phi_{p_1,1} & \cdots & \Phi_{p_1,N} \\ \cdots & \cdots & \cdots \\ \Phi_{p_N,1} & \cdots & \Phi_{p_N,N} \end{pmatrix} = \bar{x} \cdot \Phi$$

# Determinantal form can be extended to BCS wave-function of pairs with fixed particle number

Short Communication

Tome 49

N° 4

AVRIL 1988

LE JOURNAL DE PHYSIQUE

Pair wave functions for strongly correlated fermions and their determinantal representation

*J. Phys. France* 49 (1988) 553-559

AVRIL 1988, PAGE 553

J.P. Bouchaud <sup>(1)</sup>, A. Georges <sup>(2)</sup> and C. Lhuillier <sup>(1,3)</sup>

**Abstract.**— We show that a (Jastrow projected or not) BCS wave function with any fixed number of fermions can be represented as a determinant. This is important for their numerical investigation, with applications to liquid He<sup>3</sup> and Hubbard's model. We also propose a new type of wave function, describing a *mixed* state composed of paired and unpaired fermions. The physical properties of such a state are tentatively discussed.

$$|\Psi_N\rangle = \hat{P}_N |\Psi_{BCS}\rangle = \left[ \sum_k \phi_k c_{k\uparrow}^+ c_{-k\downarrow}^+ \right]^{N/2} |0\rangle = \mathcal{A}[\phi(12)\phi(34)\cdots]$$

$$\langle \{r_i^\uparrow, r_j^\downarrow\} | \Psi_N \rangle = \det [\phi(r_i^\uparrow - r_j^\downarrow)]$$

# Hartree-Fock for the 2D Hubbard model

**Incommensurate Antiferromagnetism in the Two-Dimensional Hubbard Model**

H. J. Schulz

*Laboratoire de Physique des Solides, Université Paris-Sud, 91405 Orsay CEDEX, France*

(Received 27 February 1989)

Weak coupling  
 $U/t=2$

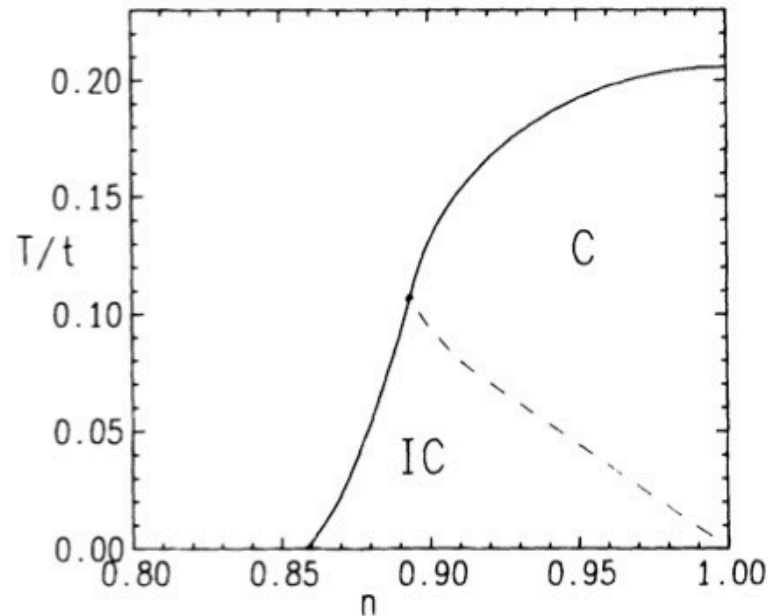


FIG. 2. Phase diagram (Ref. 14) in the temperature-density ( $n$ ) plane for  $U = 2t$ , with commensurate (C) and incommensurate (IC) antiferromagnetic phases, and the paramagnetic state. Most of the C-IC line is only schematic (see text). For  $n < n_c = 0.857$  the IC phase is metallic; for  $n > n_c$  it is insulating.

However, homogeneous SDWs are unstable against domain-wall formation (eventually leading to `stripes')

- Early Theoretical Predictions of Stripes:
- Mean-Field/Hartree-Fock
- HJ Schulz PRL64, 1445 (1990) and J.Physique 50, 2833 (1989)
- J.Zaanen and O.Gunnarsson, Phys Rev B 40, 7391 (1989)
- K.Machida, Physica C 158, 192 (1989)
- Su PRB 88, 9904 (1988); Yang and Su, PRB 44, 6838 (1991)
- Kato et al. JPSJ 59, 1047 (1990)
- M.Inui and P.Littlewood Phys Rev B 44, 4415 (1991)
- Xu et al. J.Phys Cond Mat 23, 505601 (1991)
- **Variational Monte-Carlo**: T.Giamarchi and C.Lhuillier, PRB 42, 10641 (1990)
- More advanced numerical methods (e.g. DMRG): see later slides

This is beautifully explained in:

*J. Phys. France* **50** (1989) 2833-2849

15 SEPTEMBRE **1989**, PAGE 2833

Classification

*Physics Abstracts*

75.10L — 75.25 — 75.30F



## **Domain walls in a doped antiferromagnet**

H. J. Schulz

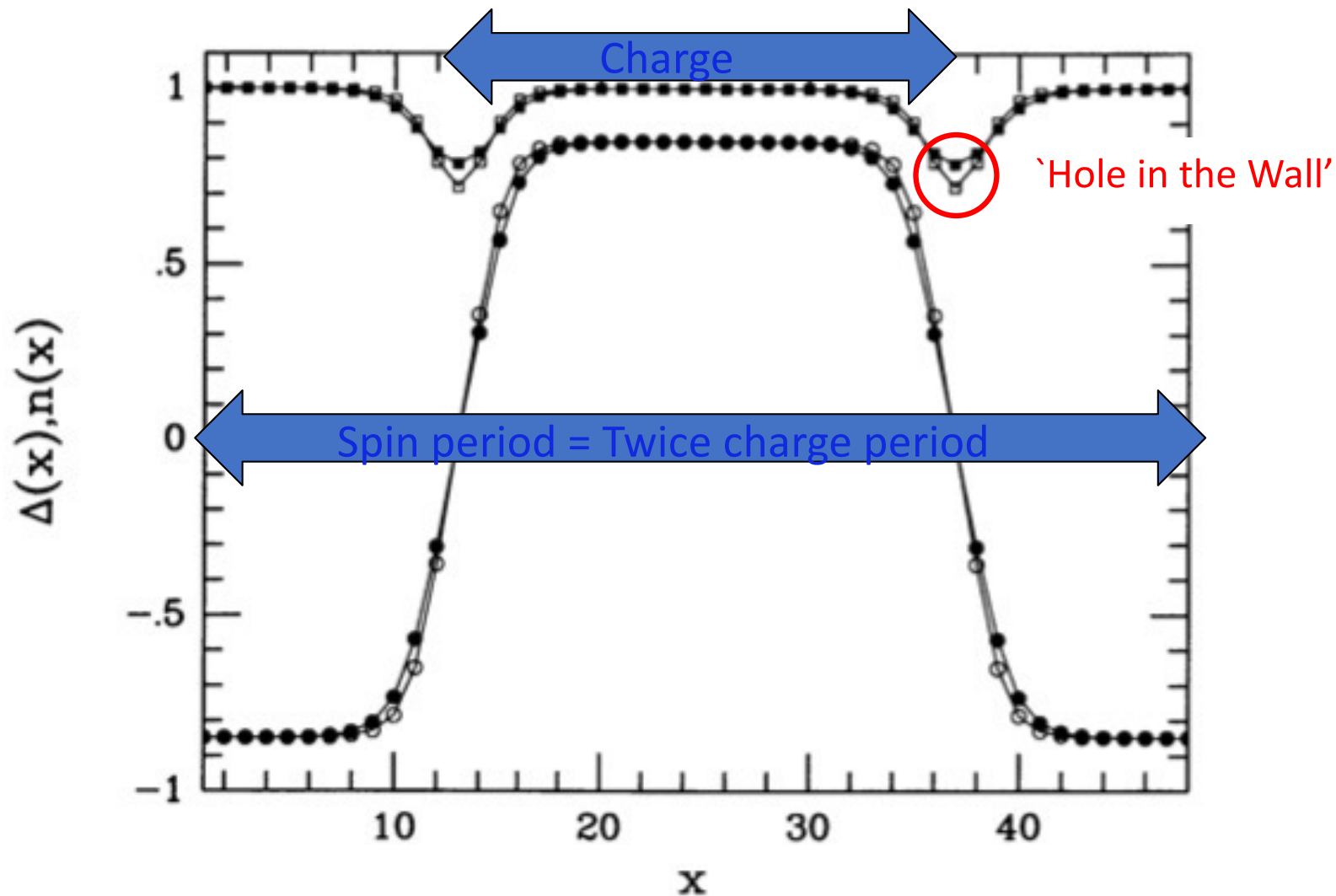
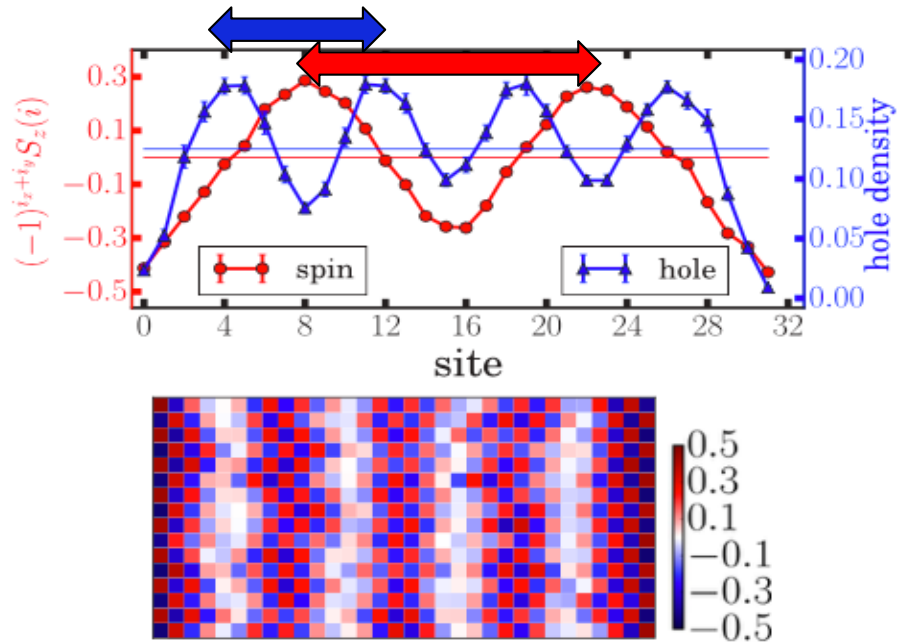


Fig. 2. — The local order parameter  $\Delta(x) = Um(x)/2$  (circles) and the electron density  $n(x)$  (squares) for a situation with two type I vertical walls, centered at  $x = 13$  and  $x = 37$ , as determined from the selfconsistent solution of the Hartree-Fock equations for  $U = 3t$ . Full and empty symbols are results with and without the charge interaction terms, respectively. Note that inclusion of the charge interactions increases the width of the walls. Even though this seems to be a small effect here, it leads to appreciable changes in energy (compare Figs. 4 and 5).

The 'classic stripe' ( $t'=0$ ): incommensurate SDW AND CDW  
 charge wavelength = spin wavelength / 2 = 1/doping (= 8 here)



Electron density  
 is largest  
 at maxima of SDW

Hole density  
 largest at nodes

FIG. 4. Converged CPMC results after a self-consistent procedure for a large system of  $16 \times 32$ . In the upper panel, the staggered spin and hole densities are plotted. The red and blue horizontal lines represent zero spin density and the average hole density, respectively. In the lower pane, the spin density for the cell is shown with a color map. As in the earlier systems,  $U = 8t$ ,  $h = 1/8$ , and a pinning field is applied to both edges along  $L_y$ .

Qin, Shi and Zhang PRB 94, 235119 (2016)  
 Auxiliary Field Constrained Path Monte Carlo

# Spin- and charge-density waves in the Hartree–Fock ground state of the two-dimensional Hubbard model

Jie Xu, Chia-Chen Chang<sup>1</sup>, Eric J Walter and Shiwei Zhang

Department of Physics, College of William and Mary, Williamsburg, VA 23187, USA

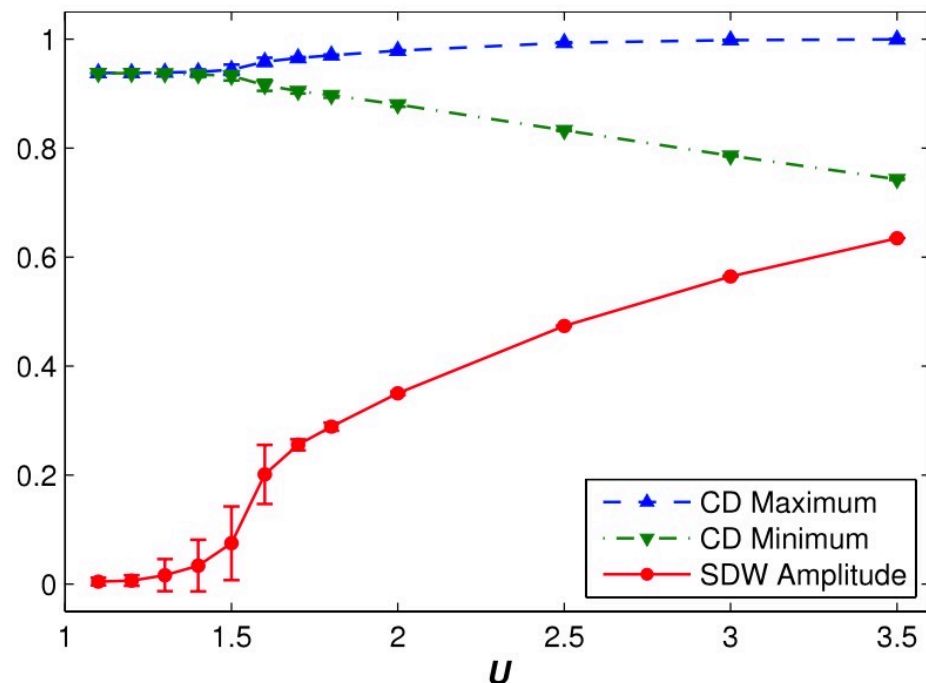


**Figure 10.** Maximum and minimum of the CD and SDW amplitude for an  $8 \times 64$  supercell with doping of  $1/16$ .

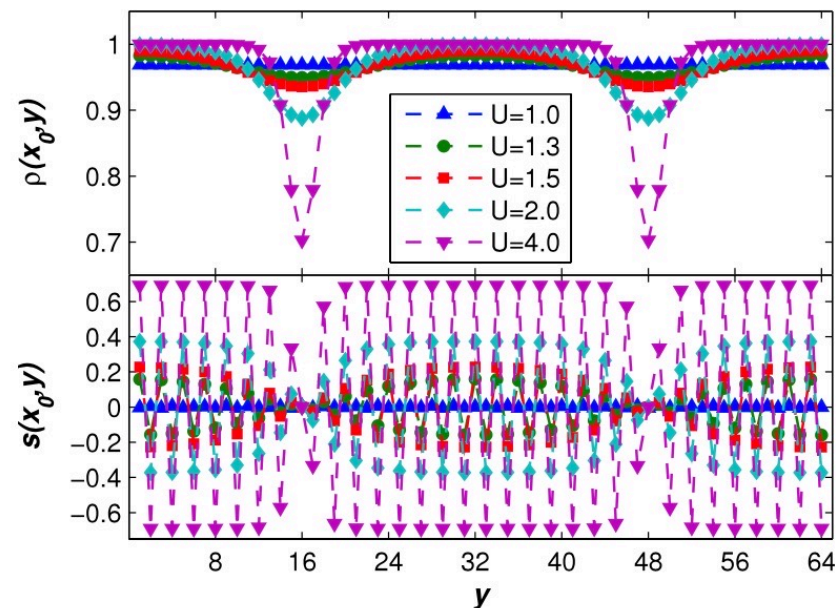


**Figure 9.** CD (top) and SD (bottom) along the  $y$ -direction versus  $U$ . The system being studied is an  $8 \times 64$  supercell with doping of  $1/32$  at  $U = 1.0, 1.3, 1.5, 2.0, 4.0$ . Each curve is a 1D cut in which the linear wave propagates. Beyond  $U_c$ , the 1-CDW and 1-SDW amplitudes increase with  $U$  and the ground state ends up in an 1-stripes state. The CDW amplitude is much weaker than that of the SDW.

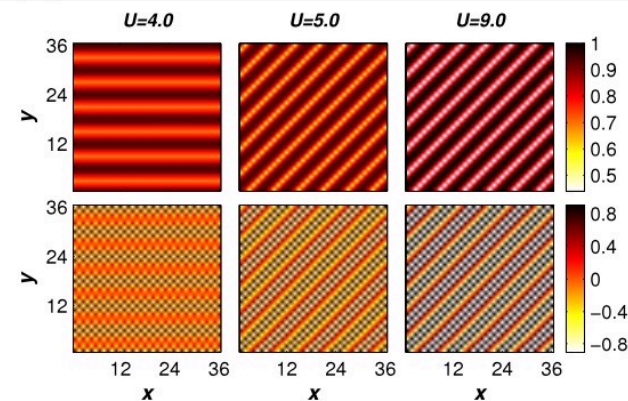


**Figure 11.** Contour plots of CD (top) and SD (bottom) versus interacting strengths. The system being studied is a  $36 \times 36$  supercell with doping of  $h = 1/6$  at  $U = 4.0, 5.0$  and  $9.0$  (from left to right), representing 1-SDW, d-SDW and d-stripes state respectively.

# Consistent with Inhomogeneous (Unrestricted) DMFT

PHYSICAL REVIEW B **89**, 155134 (2014)

## **Spin density waves in the Hubbard model: A DMFT approach**

Robert Peters<sup>1,2,\*</sup> and Norio Kawakami<sup>1</sup>

<sup>1</sup>*Department of Physics, Kyoto University, Kyoto 606-8502, Japan*

<sup>2</sup>*Computational Condensed Matter Physics Laboratory, RIKEN, Wako, Saitama 351-0198, Japan*

(Received 17 March 2014; revised manuscript received 13 April 2014; published 24 April 2014)

(

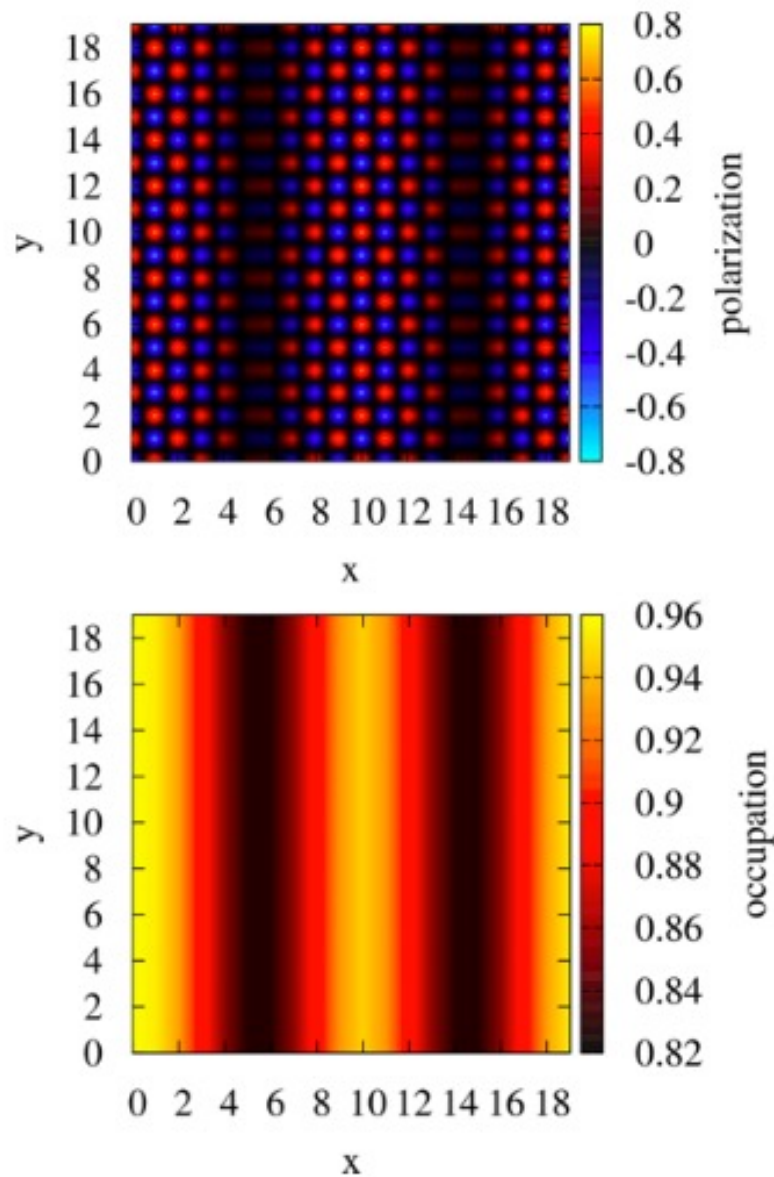


FIG. 1. (Color online) Typical pattern for a vertical SDW state in the Hubbard model for  $U = 8t$  and an average electron density  $\langle n \rangle = 0.9$ . The upper (lower) panel shows the electron polarization (density).

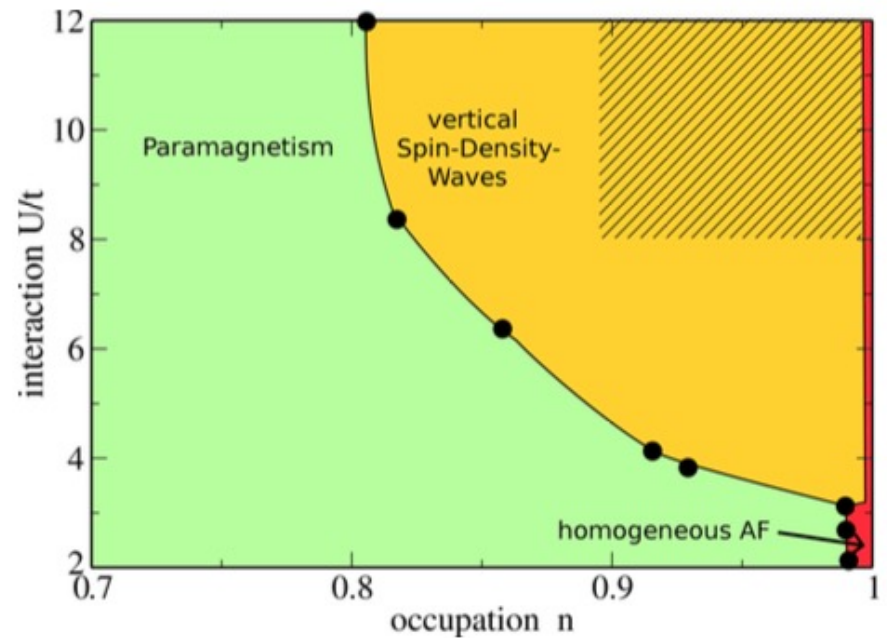


FIG. 2. (Color online) Phase diagram of the Hubbard on a square lattice as calculated by IDMFT. The shaded region represents parameters where we find vertical as well as diagonal SDWs to be stable. The homogeneous Néel state exists exactly at half filling for all interaction strengths and for a slightly doped region at weak interaction.

Peters and Kawakami  
 PRB 89, 155134 (2014)  
 Inhomogeneous DMFT  
 ( $t'=0$ )

# Comprehensive mean-field analysis of magnetic and charge orders in the two-dimensional Hubbard model

Robin Scholle,<sup>1</sup> Pietro M. Bonetti,<sup>1</sup> Demetrio Vilardi,<sup>1</sup> and Walter Metzner<sup>1</sup>

<sup>1</sup>Max Planck Institute for Solid State Research, D-70569 Stuttgart, Germany

(Dated: March 29, 2023)

Very recent  
extensive  
Hartree-Fock  
study  
(03/2023)...

arXiv:2303.15358

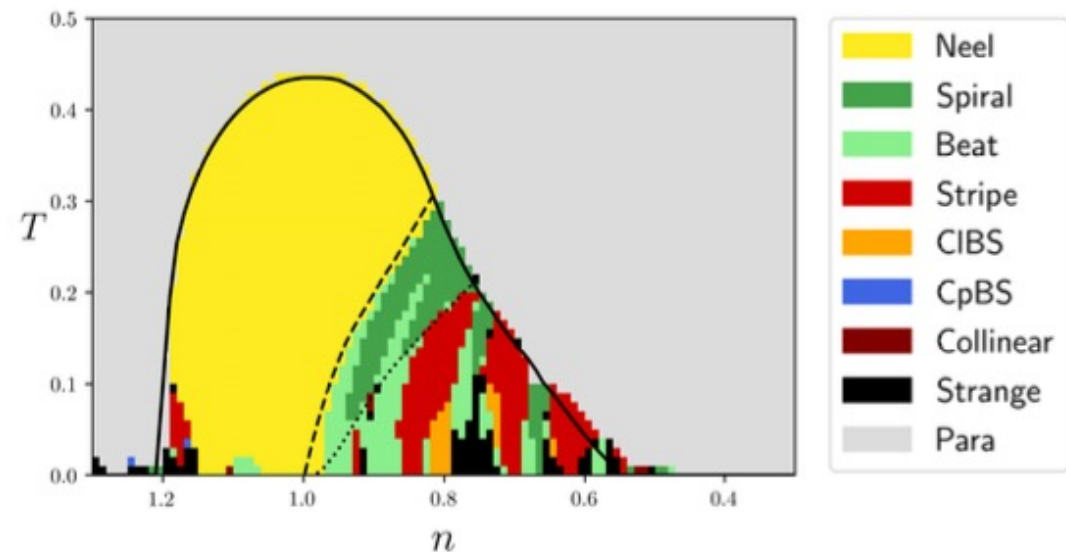


Figure 2. Phase diagram for  $U = 3t$  and  $t' = -0.15t$ . The colors label the states resulting from the real space calculation on a  $20 \times 20$  lattice. The black lines were obtained from calculations in momentum space in the thermodynamic limit. The solid black line indicates the transition temperature  $T^*$  separating the paramagnetic from the magnetically ordered regime, the dashed black line the transition between Néel and non-Néel spiral order, and the dotted black line the divergence of the charge susceptibility in the spiral state.

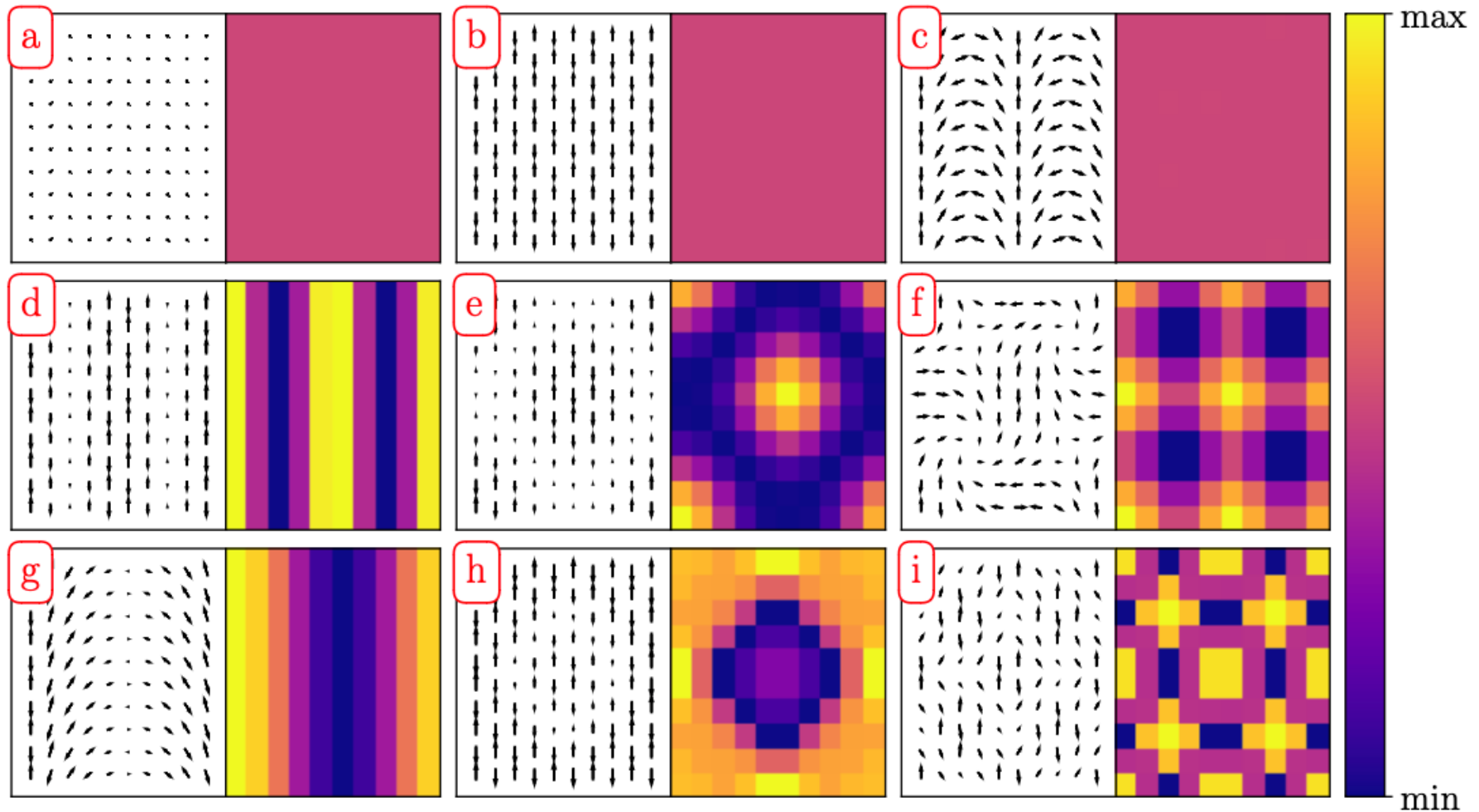


Figure 1. Overview of the different orders found in our calculations, schematically shown on a  $10 \times 10$  lattice. In each panel, the square on the left shows the relative spin orientations and amplitudes (length of the arrows) of each phase, where we chose a frame such that the spins lie the  $x$ - $y$  plane and the bottom left spin points along the  $y$ -direction. The right plot in each panel shows the corresponding charge modulation, using a color code defined on the right edge of the figure. The various panels exemplify the following magnetic orders: (a) paramagnetism, (b) Néel antiferromagnetism, (c) spiral order, (d) stripe order, (e) collinear bidirectional stripe order, (f) coplanar bidirectional stripe order, (g) beat order, (h) other collinear orders, (i) “strange” order. Only one example of strange order has been shown, while we also find different ones, often with less regular patterns.

# But in the thermodynamic limit...

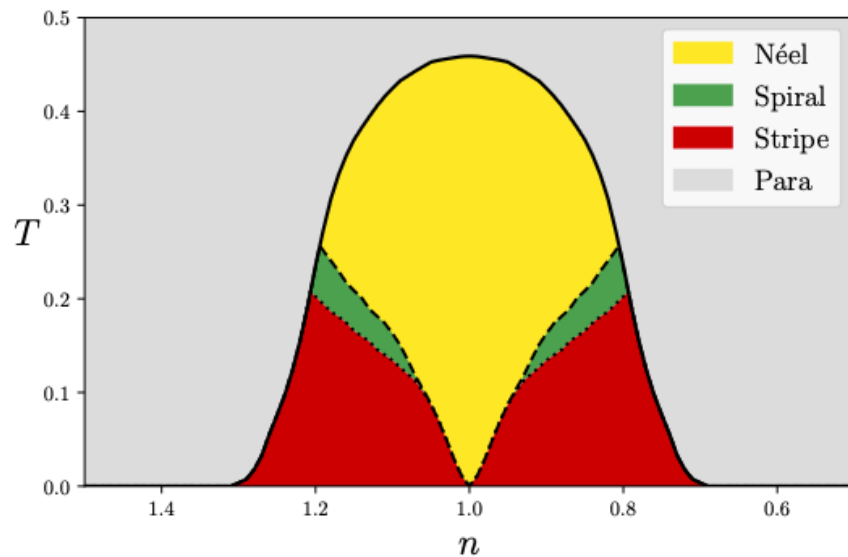


Figure 12.  $(n, T)$  phase diagram for  $t' = 0$  and  $U = 3t$  in the thermodynamic limit with Néel, spiral, and unidirectional stripe order. Because of the Hamiltonian's particle-hole symmetry, this phase diagram is symmetric.

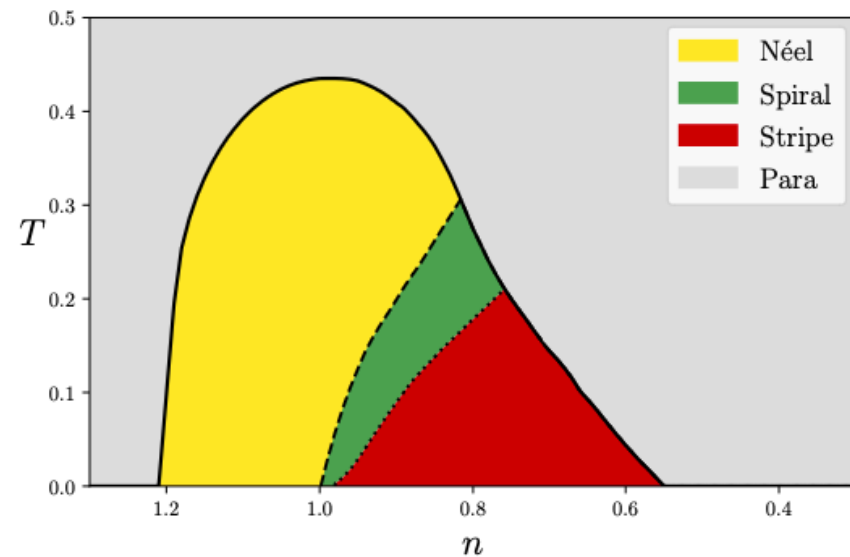


Figure 13.  $(n, T)$  phase diagram for  $t' = -0.15t$  and  $U = 3t$  in the thermodynamic limit with Néel, spiral, and unidirectional stripe order. There is a narrow spiral regime at small hole doping even at  $T = 0$ .

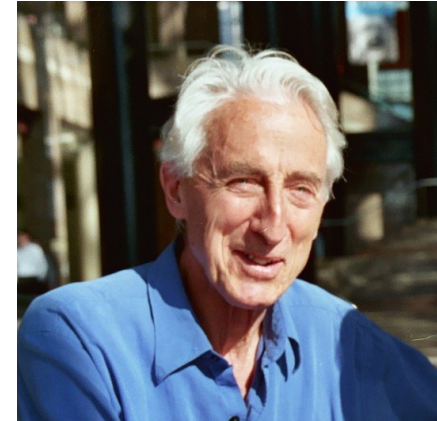
# Strengths and Limitations of Hartree-Fock

- Good indicator of some of the phases (spin, charge ordering) that can emerge
- Of course, HF must be interpreted with a generous/open mind: yes, it breaks Mermin-Wagner...
- ... But good indicator of which correlations grow first: cf. Šimkovic, Rossi and Ferrero Phys. Rev. Research 4, 043201 (2022) diagrammatic MC/CDET
- Because non-local correlations are not properly treated, NO POSSIBILITY OF non-local (e.g. d-wave) Superconductivity

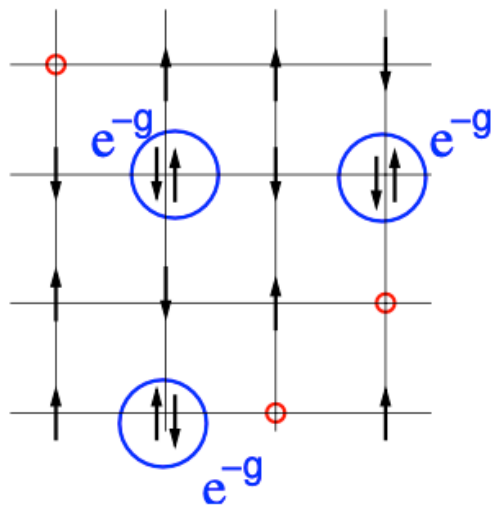
# The Gutzwiller Wave Function

$$|\Psi_G\rangle = e^{-g \sum_i \hat{n}_{i\uparrow} \hat{n}_{i\downarrow}} |\Psi_{SD}\rangle$$

$$= \prod_i [1 + (e^{-g} - 1) \hat{n}_{i\uparrow} \hat{n}_{i\downarrow}] |\Psi_{SD}\rangle$$



Martin Gutzwiller  
(1925-2014,  
Switzerland/USA)



Becca, 2019

Evaluation by  
Monte Carlo  
(beyond the Gutzwiller  
approximation):  
Yokoyama and Shiba  
JPSJ 56, 1490 1986  
JPSJ 56, 3570 1987

PRL 10, 159 (1962)

EFFECT OF CORRELATION ON THE FERROMAGNETISM OF TRANSITION METALS

Martin C. Gutzwiller

Research Laboratory Zurich, International Business Machines Corporation, Rüschlikon ZH, Switzerland  
(Received 27 September 1962)

The purpose of this Letter is to present a new approach to the problem of ferromagnetism in a metal. A correlated wave function for the electrons in the 3d band is proposed as approximation to the ground state. The expectation value of the energy is evaluated by diagram techniques. The simplest example of a face-centered cubic structure (whose density-of-states curve is parabolic at the bottom and has a peak at the top) is discussed. Under these assumptions the arguments show that the ferromagnetic state is lower if the band is nearly full, whereas the nonmagnetic state has the lower energy if the band is nearly empty.

# Limitations of the Gutzwiller wavefunction

- GWF vs. Gutzwiller approximation
- The GWF is always metallic for any (finite) value of  $g$
- Finite  $g$  unable to describe a Mott insulator without magnetic order such as Hubbard model in  $d=1$  or on a fully connected lattice with random hopping
- $N(k)$  always discontinuous at Fermi level, see e.g: W.Metzner and D.Vollhardt PRL 59, 121 (1987) and PRB 37, 7382 (1988)
- Fully projected GWF ( $g=\infty$ ) at half-filling prevents double occupancies and holes. Many applications to RVB like states (see review by C.Gros)
- Away from  $\frac{1}{2}$ -filling, fully projected GWF gives the same weight to configurations with holes and with single occupancy.

# GWF applied to Hubbard d=1

W.Metzner, D.Vollhardt PRL 59, 121 (1987)

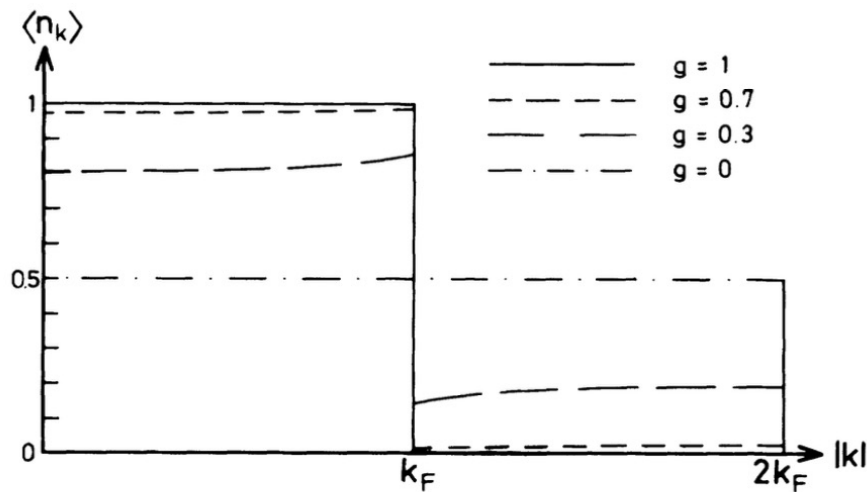


FIG. 1. The momentum distribution  $\langle n_k \rangle$  for several values of the correlation parameter  $g$  in the case of a half-filled band ( $n_\uparrow = n_\downarrow = \frac{1}{2}$ ).

Here  $g$  stands for  $e^{-g}$  of previous slide

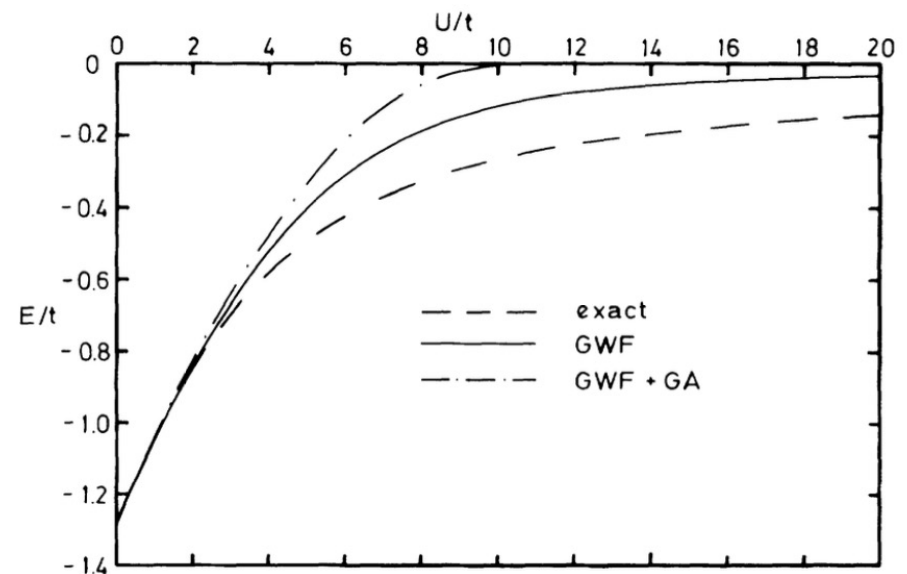


FIG. 2. The ground-state energy  $E$  for the one-dimensional Hubbard model with  $n_\uparrow = n_\downarrow = \frac{1}{2}$  as a function of  $U$ . The results for  $E$ , as calculated with the Gutzwiller wave function (GWF), are compared with the result of the Gutzwiller approximation (GWF+GA) (Ref. 23) and the exact result (Ref. 9).

# Extension of the Gutwiler wave-function to phases with broken symmetries: the come-back of stripes!

T.Giamarchi and C.Lhuillier PRB 42, 10641 (1990)

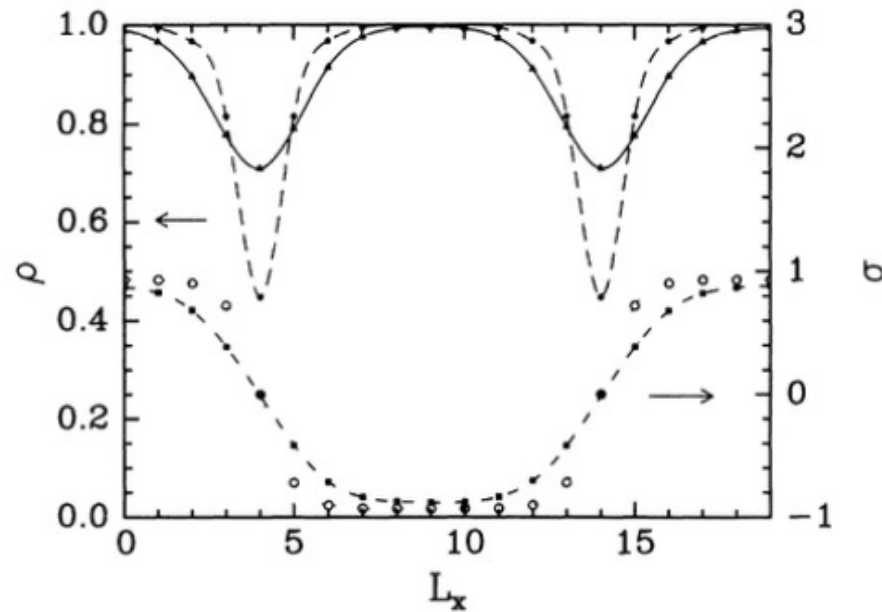


FIG. 2. Profiles of density ( $\rho$ ) and staggered magnetization ( $\sigma$ ) for two vertical domain walls (solid and dash-dotted lines), for a  $4 \times 20$  system at  $U=10$ . In dashed and dotted lines is the pure Hartree-Fock solution (obtained with the same method by fixing  $g=1$ ). The effect of the Gutzwiller prefactor is to considerably enlarge the walls. Since it weakens the Hubbard repulsion, the gain is kinetic energy associated with a larger wall supersedes the loss in magnetic energy.

Also suggested coexistence of d-wave SC and incommensurate SDW

# Variational Monte Carlo: optimization of variational wave-functions by Metropolis sampling

- Reminder from lecture 1:
- Move between configurations  $x \rightarrow x'$
- Need to evaluate:
- Ratio of probabilities  $\frac{P(x')}{P(x)} = \frac{|\psi(x')|^2}{|\psi(x)|^2}$
- For determinantal wave-functions, various tricks to make this more efficient (but does not extend to NQS)
- Local energy:  $\sum_{x'} \langle x | H | x' \rangle \frac{\psi(x')}{\psi(x)}$
- The point here is that H is a sparse matrix in configuration space because it is short-range
- Also need to calculate the metric tensor if we use NGD/stochastic reconfiguration

# Jastrow-Slater Wave Function

Continuous space: Slater determinant with (possibly long-range) symmetric weight:

$$e^{\frac{1}{2} \sum_{ij} u(r_i - r_j)} \psi_{\text{SD}}(r_1, \dots, r_N)$$

General form also applicable to lattice:

$$|\Psi_{\text{JS}}\rangle = e^{\frac{1}{2} \sum_{pq} g_{pq} \hat{n}_p \hat{n}_q} |\Psi_{\text{SD}}\rangle$$
$$(1 \leq p, q \leq M)$$

## Variational Description of Mott Insulators

Manuela Capello,<sup>1,2</sup> Federico Becca,<sup>1,2</sup> Michele Fabrizio,<sup>1,2,3</sup> Sandro Sorella,<sup>1,2</sup> and Erio Tosatti<sup>1,2,3</sup>

<sup>1</sup>International School for Advanced Studies (SISSA), Via Beirut 2-4, I-34014 Trieste, Italy

<sup>2</sup>INFM-Democritos National Simulation Centre, Trieste, Italy

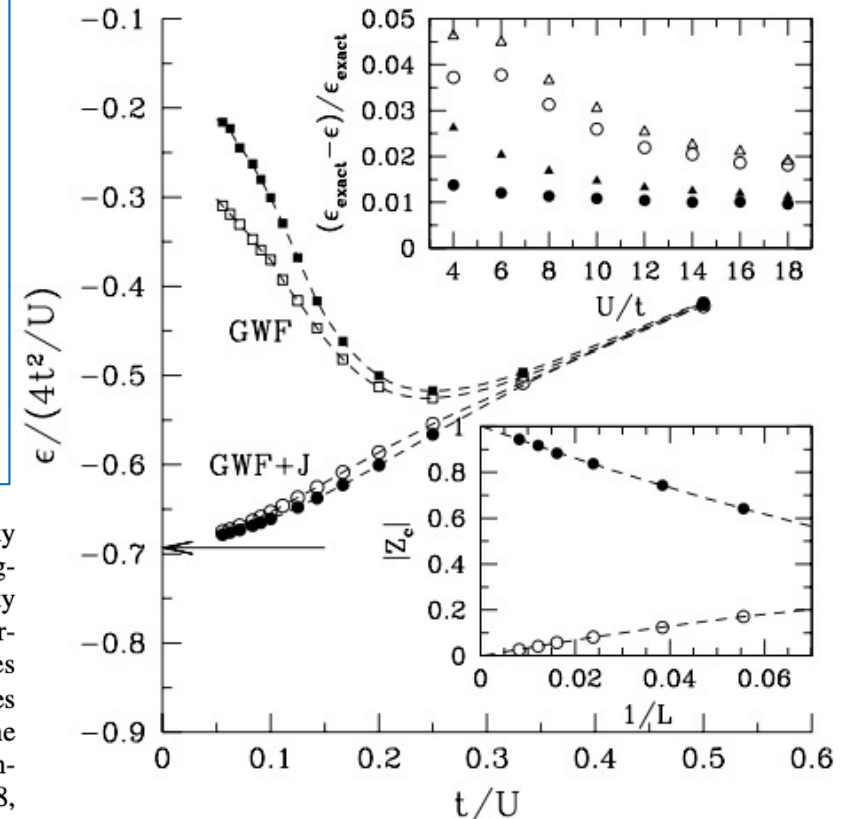
<sup>3</sup>International Centre for Theoretical Physics (ICTP), P.O. Box 586, I-34014 Trieste, Italy

(Received 17 March 2004; published 20 January 2005)

The Gutzwiller wave function for a strongly correlated model can, if supplemented with a long-range Jastrow factor, provide a proper variational description of Mott insulators, so far unavailable. We demonstrate this concept in the prototypical one-dimensional  $t - t'$  Hubbard model, where at half-filling we reproduce all known phases, namely, the ordinary Mott undimerized insulator with power-law spin correlations at small  $t'/t$ , the spin-gapped metal above a critical  $t'/t$  and small  $U$ , and the dimerized Mott insulator at large repulsion.

- JSWF applied to Hubbard model in  $d=1$
- In contrast to GWF, able to reproduce Mott insulator at  $\frac{1}{2}$ -filling (with no symmetry breaking)
- Long-range Jastrow crucial
- $d=2$ : JSWF is not enough see: Capello et al PRB 73, 245116 (2006)

FIG. 2. Energy per site  $\epsilon$  for the simple GWF ( $L = 18$ , empty squares, and  $L = 82$ , full squares) and for the WF with long-range density-density Jastrow (GWF + J) ( $L = 18$ , empty circles, and  $L = 82$ , full circles), for  $t' = 0$ . The Slater determinant is a simple Fermi sea, with  $\Delta_q = 0$ . The arrow indicates the exact energy per site of the Heisenberg model, and the lines are guides to the eye. Top inset: accuracy of the WF with all the density-density Jastrow independently minimized (same symbols as before) and with the analytic parametrization ( $L = 18$ , empty triangles, and  $L = 82$ , full triangles). Bottom inset:  $Z_c$  for the GWF + J (full circles) and for the GWF (open circles); lines are three parameter fits.



# 'Backflow'

- General idea: allow the 1-particle orbitals entering the Slater determinant
- to depend on the coordinates on all other particles.
- First proposed in the continuum (Helium 4) by Feynman and Cohen  
Phys Rev 102, 1189 (1956)
- Applied to the lattice only in 2008 and onwards:  
Tocchio et al. PRB 78, 041101 (2008); PRB 83, 185138 (2011);  
PRB 94, 195126 (2016)

$$\bar{\mathbf{r}}_1 = b(\mathbf{r}_1; \mathbf{r}_2, \dots, \mathbf{r}_N) , \text{ etc.}$$

$$\psi_{\text{SD}}(r_1, \dots, r_N) = \det [\phi_{\alpha_i}(\bar{r}_j)]$$

For example:  $\phi_{\alpha}(\bar{r}_i) = \phi_{\alpha}(r_i) + \sum_j c_{ij}[x] \phi_{\alpha}(r_j)$

More generally:

$$\det \begin{bmatrix} \Phi_{x_1,1}[n(x)] & \dots & \Phi_{x_1,N}[n(x)] \\ \vdots & \ddots & \vdots \\ \Phi_{x_N,1}[n(x)] & \dots & \Phi_{x_N,N}[n(x)] \end{bmatrix}$$

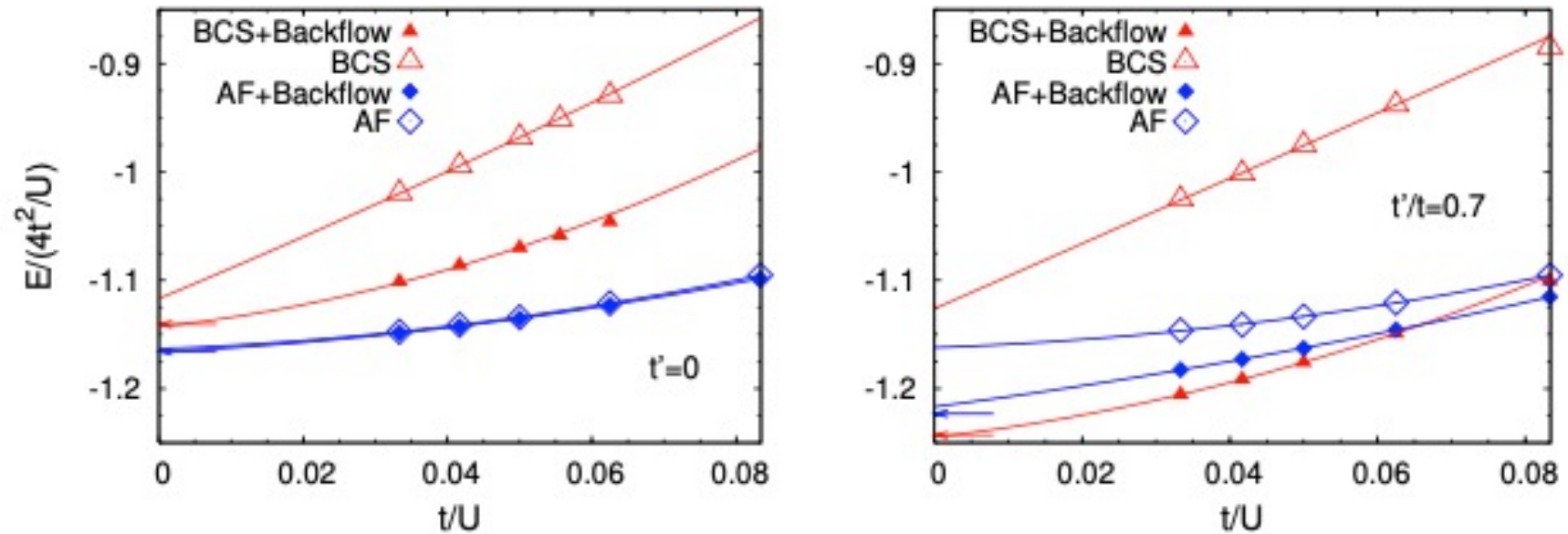


**Fig. 2:** Energies per site (in units of  $J = 4t^2/U$ ) for the two-dimensional Hubbard model at half filling, for both the unfrustrated ( $t' = 0$ ) and frustrated ( $t'/t = 0.7$ ) case. The cases with and without backflow correlations are reported (for the BCS state). The results for the wave function with antiferromagnetic order and no BCS pairing are also shown. Arrows indicate the energies per site for the corresponding fully-projected states in the Heisenberg model.

## Hidden Mott transition and large- $U$ superconductivity in the two-dimensional Hubbard model

Luca F. Tocchio, Federico Becca, and Sandro Sorella

*CNR-IOM-Democritos National Simulation Centre and International School for Advanced Studies (SISSA),  
Via Bonomea 265, I-34136, Trieste, Italy*

(Received 29 July 2016; revised manuscript received 26 September 2016; published 14 November 2016)

We consider the one-band Hubbard model on the square lattice by using variational and Green's function Monte Carlo methods, where the variational states contain Jastrow and backflow correlations on top of an uncorrelated wave function that includes BCS pairing and magnetic order. At half-filling, where the ground state is antiferromagnetically ordered for any value of the on-site interaction  $U$ , we can identify a hidden critical point  $U_{\text{Mott}}$ , above which a finite BCS pairing is stabilized in the wave function. The existence of this point is reminiscent of the Mott transition in the paramagnetic sector and determines a separation between a Slater insulator (at small values of  $U$ ), where magnetism induces a potential energy gain, and a Mott insulator (at large values of  $U$ ), where magnetic correlations drive a kinetic energy gain. Most importantly, the existence of  $U_{\text{Mott}}$  has crucial consequences when doping the system: We observe a tendency for phase separation into hole-rich and hole-poor regions only when doping the Slater insulator, while the system is uniform by doping the Mott insulator. Superconducting correlations are clearly observed above  $U_{\text{Mott}}$ , leading to the characteristic dome structure in doping. Furthermore, we show that the energy gain due to the presence of a finite BCS pairing above  $U_{\text{Mott}}$  shifts from the potential to the kinetic sector by increasing the value of the Coulomb repulsion.

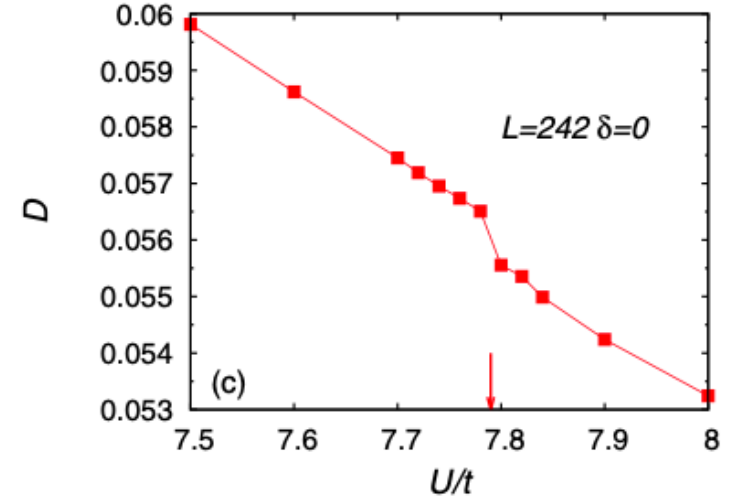
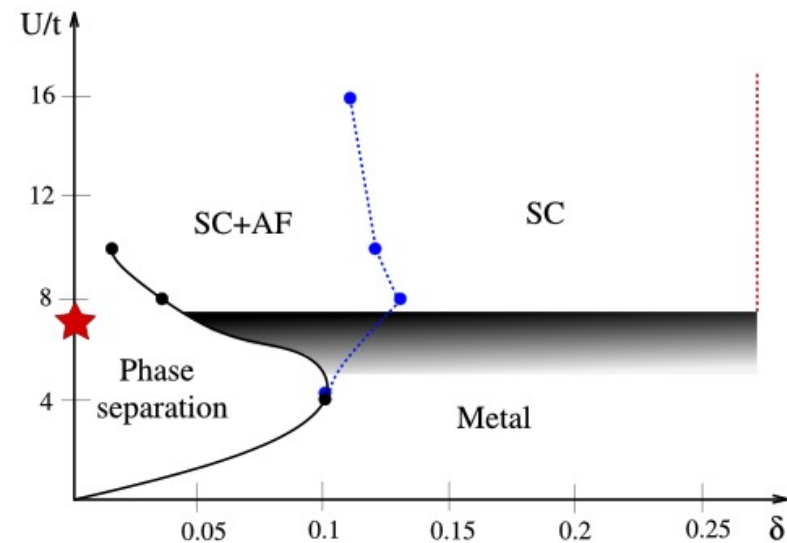


FIG. 7. Schematic phase diagram as obtained by using a combined VMC and GFMC (with FN approximation) approach. The red star labels the location of the hidden Mott transition  $U_{\text{Mott}}/t$  at half-filling. The black line with black dots denotes the boundary of the phase-separation region, that shrinks for  $U/t \gtrsim U_{\text{Mott}}/t$ . The curve is left open for  $U/t > 10$ , since we cannot exclude the presence of phase separation very close to half-filling. The dashed blue line with blue dots marks the disappearance of  $\Delta_{\text{AF}}$  in the optimal variational state. The dashed red line indicates the boundary of the region where sizable pairing correlations are detected. Finally, in the shaded gray region finite-size effects are strong and precise results cannot be obtained in the thermodynamic limit.



Overview:

Despite obvious successes, variational MC is limited by the flexibility of the parametrized form of the wave-function

→ This is where NNs as 'universal approximators' less biased than humans 😊 can make a difference

Dawn of a New Era  
for Fermionic Variational Wave  
Functions:  
Neural Quantum States and ML

→ Lecture 5, May 30

ARTICLE Nature Communications, 2018

DOI: 10.1038/s41467-018-06598-z OPEN

## Quantum machine learning for electronic structure calculations

Rongxin Xia<sup>1</sup> & Sabre Kais<sup>1,2,3</sup>

Some examples:  
(we'll focus especially on  
Hidden Fermions on May 30)

15724-9

OPEN

Nature Communications, 2020

## Fermionic neural-network states for ab-initio electronic structure

Kenny Choo<sup>1</sup>, Antonio Mezzacapo<sup>2</sup> & Giuseppe Carleo<sup>3</sup>

'FermiNet'

PHYSICAL REVIEW RESEARCH 2, 033429 (2020)

### *Ab initio* solution of the many-electron Schrödinger equation with deep neural networks

David Pfau,<sup>\*,†</sup> James S. Spencer,<sup>\*</sup> and Alexander G. D. G. Matthews  
*DeepMind, 6 Pancras Square, London NIC 4AG, United Kingdom*

W. M. C. Foulkes<sup>Ⓜ</sup>

*Department of Physics, Imperial College London, South Kensington Campus, London SW7 2AZ, United Kingdom*

**PNAS**

RESEARCH ARTICLE | PHYSICS

OPEN ACCESS



PNAS 2022 Vol. 119 No. 32 e2122059119

## Fermionic wave functions from neural-network constrained hidden states

Javier Robledo Moreno<sup>a,b,1</sup>, Giuseppe Carleo<sup>c,d</sup>, Antoine Georges<sup>a,e,f,g</sup>, and James Stokes<sup>a,h</sup>